A Discrete RMRAC-STSM Controller for Current Regulation of Three-Phase Grid-Tied Converters with LCL filter

Guilherme V. Hollweg
Federal University of Santa Maria
email: guilhermehollweg@gmail.com

Paulo J. D. de O. Evald
Franciscan University
email:paulo.evald@gmail.com

E. Mattos, R. V. Tambara
and H. A. Gründling
Federal University of Santa Maria

***Abstract*—This article presents a discrete robust adaptive control structure, gathering a Robust Model Reference Adaptive Controller (RMRAC) with an adaptive Super-Twisting Sliding Mode (STSM) controller. The resulting control structure is applied to current control of a voltage-fed three-phase inverter, connected to the grid by an LCL filter. The main contribution of this control proposal is its adaptability, maintaining the robustness characteristics of the controllers that compose it with good regulation performance. Moreover, as the adaptive Sliding Mode action is high-order (Super-Twisting), the chattering phenomenon is significantly mitigated. Thereby, its implementation is simplified, using a first order reference model. For this, the dynamics of the LCL filter capacitors are neglected during the modeling process, considering it as an additive unmodeled dynamics. To validate the viability of the proposed control structure, Hardware in the Loop (HIL) results are presented.**

***Keywords* – Adaptive Sliding Mode Controller, Robust Model Reference Adaptive Controller, Grid-tied Converter, LCL filter, Hardware in the Loop.**

I. Introduction

In recent years, world energy consumption is increasing, contributing to the exhaustion of natural energy reserves and consequently creating a run for new renewable energy sources. In this way, there is a popularization of micro and mini generation [1]. To use energy from a renewable source, it is necessary to convert continuous to alternate energy. For this purpose, a DC-AC converter is normally used [1]. For attenuation of the harmonic distortion present at the Point of Common Coupling (PCC) between the inverter and the electrical grid, as well as for attenuation of the high frequency harmonic components generated by the full bridge key switching, output filters are fundamental parts of grid-tied structures. The attenuation of these harmonic components is necessary for the system to meet the IEEE 1547-2018 standard, which limits injected current THD (Total Harmonic Distortion). Therefore, for good power quality, L or LCL filters are commonly used to connect the inverter to the electrical grid [2]. An L filter satisfactorily fulfills the function of suppressing harmonics, as required by current standards. However, due to its size and high cost, its use in power systems greater than 1 kW is not a viable alternative [2], making the LCL filter a better option [2], [3].

In addition to choosing a suitable output filter, another important issue in the design of a grid-tied DC-AC converter is the robustness of the current controller, since the inductance of the electrical grid is uncertain [4], [5]. Note that its impedance varies depending on local energy system quality, and may have a high inductive content (weak grid). The inductive content of the electrical grid is a challenge for control system, since it drastically increases the required controller efforts to keep the system stable and with the currents properly regulated [4].

The current control of a DC-AC converter with LCL filter has already been implemented using several control techniques, such as: Proportional-Integral Controller [3], P+R (Proportional+Resonant) Controllers [6], Robust Quadratic Linear Regulator [7], Robust Model Reference Adaptive Controller (RMRAC) [4], modified RMRAC [8], among others. Also, recently [9] proposed a robust P+R with a first order Sliding Mode (SM) controller. However, control structures that use sliding mode terms usually presents chattering, generated due to their high frequency non-linear action, as shown in [10] and [11]. It is noteworthy that chattering phenomenon can cause instability in the control system and problems with electromagnetic interference [11]. An alternative to mitigate chattering is to use higher-order Sliding Mode controllers, such as Super-Twisting, proposed in [10], [12]-[13], which maintains a good regulation performance and provides a significant mitigation of these persistent oscillations.

Thereby, this paper proposes the development and application of a discrete-time Robust Model Reference Adaptive Controller (RMRAC) with an adaptive Super-Twisting Sliding Mode (STSM) controller, called RMRAC-STSM. The controller is applied for current control of a three-phase grid-tied Voltage Source Inverter (VSI) connected to the electrical grid through an LCL filter. Also, the proposed controller uses a reduced-order reference model. For this purpose, a simplified model of the LCL filter is considered, where the dynamics of the LCL capacitor are neglected (equivalent to the pair of complex conjugated poles in the complete plant model), as presented in [14]. Then, the controller is robust to unmodelled dynamics. Besides, the digital implementation of the controller becomes simpler, once that a reduced order system require less parameters to adapted, impacting directly on the computational cost.

https://doi.org/10.53316/sepoc2021.033

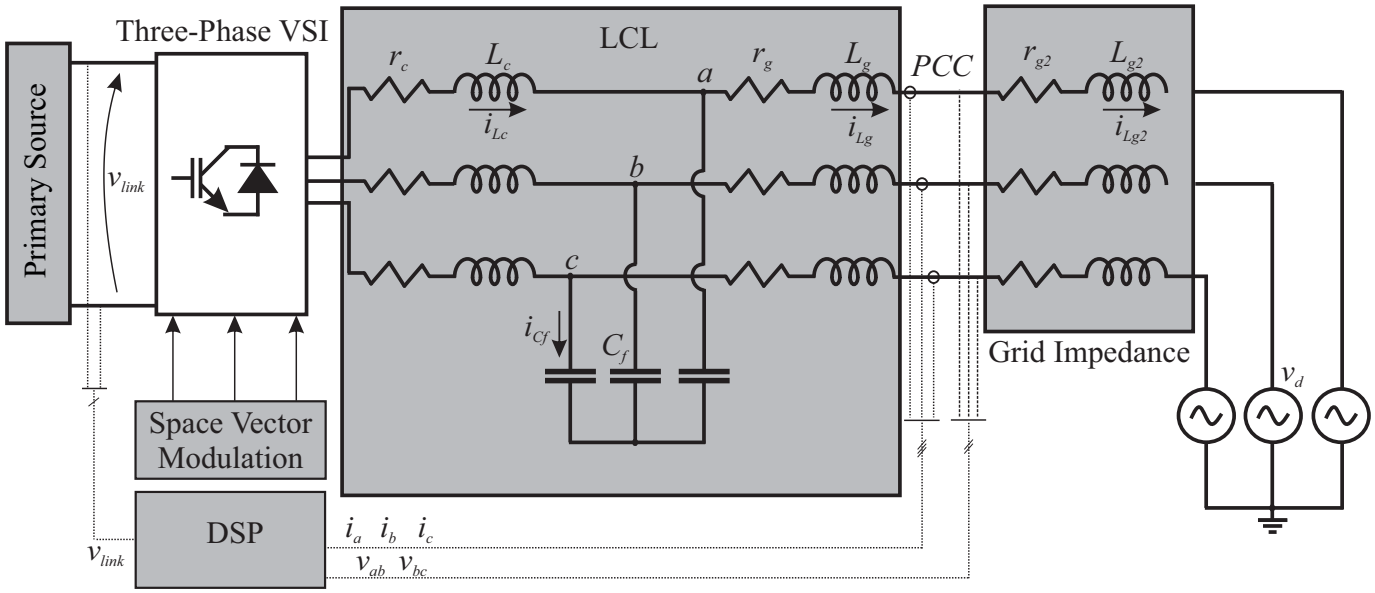

Figure 1. Three-phase grid-tied VSI with LCL filter.

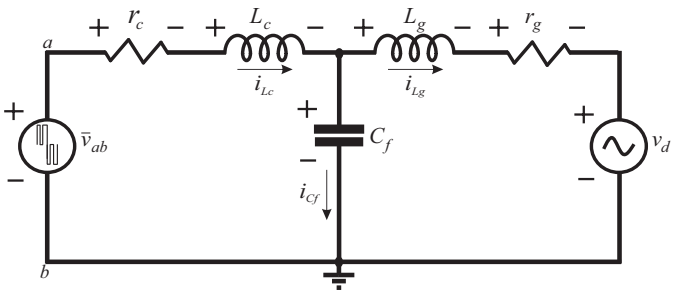

Figure 2. Single-Phase LCL equivalent circuit for modeling.

II. Plant Modeling

This section presents the LCL transfer functions in continuous and discrete-time, as well as the DC-AC converter parameters design.

A. LCL Transfer Functions

The three-phase grid-tied VSI diagram is shown on Figure 1, where r_c and L_c constitute the inverter-side impedance, r_g and L_g constitute the grid-side impedance and C_f are the LCL filter capacitors. Note that r_{g_2} and L_{g2} constitutes the electrical grid impedance, unknown in the LCL modeling, since they change according to local grid characteristics [4]. Moreover, V_{link} is the primary source and v_d represents the grid voltage. Furthermore, v_{ab} and v_{bc} are the measured line voltages and i_a, i_b and i_c are the measured phase currents. In addition, i_{Lc}, i_{Cf} and I_{Lg2} are the inverter-side, capacitor and grid-side currents, respectively. Also, the control action is synthesized using a Space Vector Modulation in order to update the inverter switches S_1 to S_6. The 3-wire grid-tied VSI with LCL filter modeling is well discussed on [4], then, the plant modeling will be briefly discussed in this paper. To ensure synchronization between converter and electrical grid, a Kalman filter, proposed in [15], is utilized.

To control the grid-injected currents, the three-phase system, in abc coordinates, is transformed into two identical decoupled single-phase models, in $\alpha\beta 0$ coordinates, using Clarke transformation, once that control design on abc coordinates is complex due to the strong model coupling [4]. Figure 2 shows the single-phase equivalent circuit.

Thus, according to [4], considering the LCL equivalent circuit shown on Figure 1, applying Kirchhoff's circuit laws and using the state-space modeling presented on [16], the continuous-time transfer function that relates the electrical grid injected current (i_{Lg}) and the modulated voltage synthesized by converter ($\bar{v}_{ab}$) can be obtained. The LCL transfer function for filter output current control can be expressed on (1),

$$\frac{i_{Lg}(s)}{\bar{v}_{ab}(s)} = \frac{\frac{1}{L_g L_c C_f}}{s^3 + \frac{(R_g L_c + R_c L_g)}{L_g L_c} s^2 + \frac{(L_c + L_g + R_g R_c C_f)}{L_g L_c C_f} s + \frac{R_g + R_c}{L_g L_c C_f}}, \quad (1)$$

where $\bar{v}_{ab}$ is the voltage synthesized by converter through the desired modulation technique.

B. Converter Parameters Design

The design of the LCL elements was made according to [2], following the proposed restrictions and steps for design. The obtained values for the LCL filter are: $L_c = 1\ mH$, $C_f = 62\ \mu F$ and $L_g = 0.3\ mH$, considering $r_c = r_g = 50m\Omega$. Also, the power inverter is $P_{in} = 5400\ W_{pk}$. Moreover, the switching frequency and sampling period are $f_s = 10.02\ kHz$ and $T_s = 99.8\ \mu s$, respectively. In addition, the DC link is $V_{link} = 500\ V$ and the electrical grid parameters are unknown.

III. RMRAC-STSM Controller

In this section, it is presented the reference model design, the proposed controller theory and the steps for its implementation.

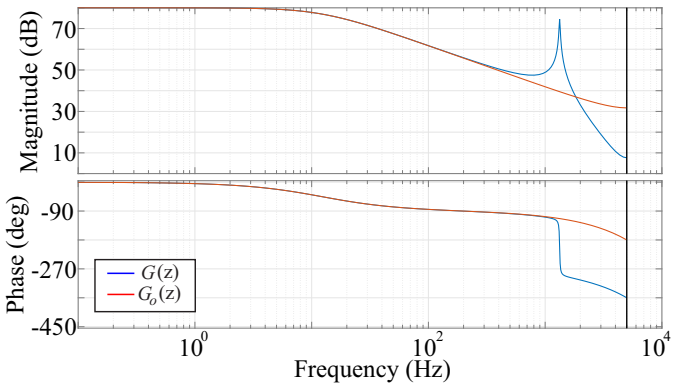

Figure 3. Bode diagram of complete plant $G(z)$ and simplified plant $G_o(z)$.

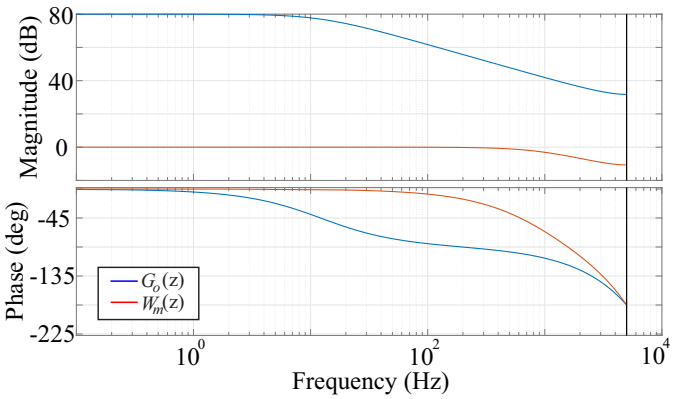

Figure 4. Bode diagram of reference model $W_m(z)$ and simplified plant $G_o(z)$.

A. Reference Model Design

Replacing the converter parameters in (1) and using a ZOH method for discretization, (2) can be obtained

$$G_{(i_{Lg},D)}(z) = G(z) = \frac{d_2 z^2 + d_1 z + d_0}{c_3 z^3 + c_2 z^2 + c_1 z + c_0}, \tag{2}$$

where $d_2 = 60.33$, $d_1 = 205.7$, $d_0 = 59.03$, $c_3 = 1$, $c_2 = -0.8119$, $c_1 = 0.8024$ and $c_0 = -0.9579$.

The discrete-time transfer function of the plant, presented in (2), has third order, which implies on a complex adaptive control system with a great set of mathematical equations that requires an elevated computational capacity from micro-controller to execute it. In order to simplify the design and implementation of the adaptive control structure, a simplified plant is considered, whose its model is a first order transfer function. This simplified plant has the same dynamics in the frequencies of interest (low frequencies) as the original plant. Thereby, the LCL resonance peak is disregarded in the simplified plant, as it occurs in high frequency, close to the Nyquist frequency. Then, the LCL complex conjugated pole pair, which represents mainly the capacitor dynamics, is considered as an unmodeled dynamics, as presented in [14]. The simplified model plant is

$$G_{(i_{Lg},D)}(z)^* = G_o(z) = \frac{151.8}{(z - 0.9849)}, \tag{3}$$

where * represents the simplification.

Figure 3 shows the Bode diagram of complete, (2), and simplified plant, (3). Thereby, considering the simplified plant model, a reference model with first order can be chosen, since its transfer function must present the same relative degree as the modeled part of the real plant. The adopted reference model is

$$W_m(z) = \frac{0.7301}{(z - 0.2699)}. \tag{4}$$

Figure (4) presents a Bode diagram of the simplified plant and the reference model. For the choice of $W_m(z)$, a gain of 0dB was considered at low frequencies and a bandwidth at least one decade greater than that of the simplified plant, in order to ensure a fast dynamic response to the adaptive structure in the regulation of converter output currents.

Note that the pair of complex conjugated poles present in the system, at high frequency, has been neglected. Therefore, the RMRAC-STSM control structure treats the complex poles of the LCL filter as an umodeled dynamic and must be robust enough to regulate the system considering this simplification, as shown in [14].

B. Control Law and Adaptive Control Algorithms

The control law is shown on (5), according to [17],

$$\boldsymbol{\theta}(k)^T \boldsymbol{\omega}(k) + r(k) = 0, \tag{5}$$

where the adaptive vector is $\boldsymbol{\theta}(k)^T = [\ \theta_u(k)\ \theta_y(k)\ \theta_{\text{SM}}(k)\ ]$ and the auxiliary vector is $\boldsymbol{\omega}(k) = [\ u(k)\ y(k)\ u_{STSM}(k)]$. Besides, $\theta_u(k)$ and $\theta_y(k)$ are the adaptive parameters from RMRAC using a first order reference model and $\theta_{SM}(k)$ is the adaptive gain from Sliding Mode. Also, $u(k)$ ($u(k) = u_{RMRAC}(k) + u_{STSM}(k)$) is the complete control action, $y(k)$ is the plant output and $u_{STSM}(k)$ is the SM control action.

Making the appropriate multiplications in (5), the u_{RMRAC} and u_{STSM} control laws can be obtained. The RMRAC control law is

$$u_{RMRAC}(k) = -\frac{\theta_y(k)}{\theta_u(k)} y(k) - \frac{1}{\theta_u(k)} r(k), \tag{6}$$

and the STSM control law is

$$u_{STSM}(k) = \frac{\theta_{SM}(k)}{\theta_u(k)} u_{SM}(k), \tag{7}$$

where $u_{SM}(k) = k_1 \sqrt{|e_1(k)|} sgn(e_1(k)) + v(k)$, and sgn is a signal function. Moreover, $v(k)$ is shown on (8), according to [10],

$$v(k) = -k_2 T_s sgn\left(e_1(k)\right) + v(k-1), \tag{8}$$

where T_s is the sample period, k_1 and k_2 are the constants from Super-Twisting Sliding Mode, both defined by the designer. Furthermore, e_1 is the tracking error, $e_1(k) = y(k) - y_m(k)$.

The adaptive algorithm is based on Gradient method. Then, the $\boldsymbol{\Gamma}$ matrix has fixed gains. In addition, the augmented error $\epsilon(k)$ is defined on (9),

$$\epsilon(k) = y(k) + \boldsymbol{\theta}(k)^T \boldsymbol{\zeta}(k), \tag{9}$$

where $\boldsymbol{\zeta}$ is an auxiliary filter (first order), responsible for filtering the adaptation parameters by the reference model, $\boldsymbol{\zeta} = W_m(z)\boldsymbol{\omega}$.

The adaptive parameter recursive equation is defined on (10),

$$\boldsymbol{\theta}(k) = \boldsymbol{\theta}(k-1)\left[1 - T_s\gamma\sigma(k-1)\right] - \frac{T_s\gamma\boldsymbol{\zeta}(k-1)\epsilon(k-1)}{m^2(k-1)}. \tag{10}$$

Note that the adaptive algorithm objective is to minimize the augmented error ϵ, expressed in (9). However, as the augmented error is correlated with the tracking error, once the augmented error is small, the system is tracking the reference and consequently the tracking error (e_1) tends to be small [17].

To incorporate robustness and limitation of all closed loop signals, a majorant signal $\bar{m}^2$ is considered, as (11)

$$\bar{m}^2(k) = m^2(k) + \boldsymbol{\zeta}^T(k)G\boldsymbol{\zeta}(k), \tag{11}$$

where G is the majorant gain, also defined by the designer. Moreover, to increase controller robustness a *σ-modification* is included [17], which avoids parameters drifting. Note that this function avoids parametric divergence, acting according to the norm of gains in each iteration,

$$\sigma(k) = \begin{cases} 0 & \text{if} \quad \|\boldsymbol{\theta}(k)\| \leq M_0 \\ \sigma_0(\frac{\|\boldsymbol{\theta}(k)\|}{M_0} - 1) & \text{if} \quad M_0 < \|\boldsymbol{\theta}(k)\| < 2M_0, \\ \sigma_0 & \text{if} \quad \|\boldsymbol{\theta}(k)\| \geq 2M_0 \end{cases} \tag{12}$$

where σ_0 is the superior limit from sigma function, M_0 is the positive parameter, which can safely be over-sized to twice the value of the norm for ideal gains, $\boldsymbol{\theta}^*$ (convergence values in steady state) [14].

The control system (5)-(12) are generic and can be applied to any plant whose modeled part is represented by a transfer function with unitary relative degree. However, for the application of the controller in the proposed plant (grid-tied three-phase VSI with LCL filter), the grid dynamics still need to be included in the system, in order to reject exogenous disturbances.

C. Periodic disturbance dynamics modeling

For the control system application on three-phase injected currents into the electrical grid by the VSI converter with LCL filter, the dynamics of electrical grid voltage can be considered as an exogenous and periodic disturbance [4], [8]. Therefore, two new adaptive parameters were added referring to the periodic disturbance (θ_c and θ_s). Also, two new signals are included in $\boldsymbol{\omega}$, $sin(k)$ and $cos(k)$, corresponding to phase and quadrature, respectively, both obtained using the Kalman Filter, as proposed in [15]. Then, the control law can be rewritten as

$$\boldsymbol{\theta}(k)^T\boldsymbol{\omega}(k) + r(k) = 0, \tag{13}$$

where $\boldsymbol{\theta}(k)^T = [\ \theta_u(k)\ \ \theta_{\mathrm{y}}(k)\ \ \theta_{\mathrm{SM}}(k)\ \ \theta_c(k)\ \ \theta_s(k)\ ]$ and the auxiliary vector can be expressed as $\boldsymbol{\omega}(k) = [\ u(k)\ y(k)\ u_{STSM}(k)\ sin(k)\ cos(k)\ ]$.

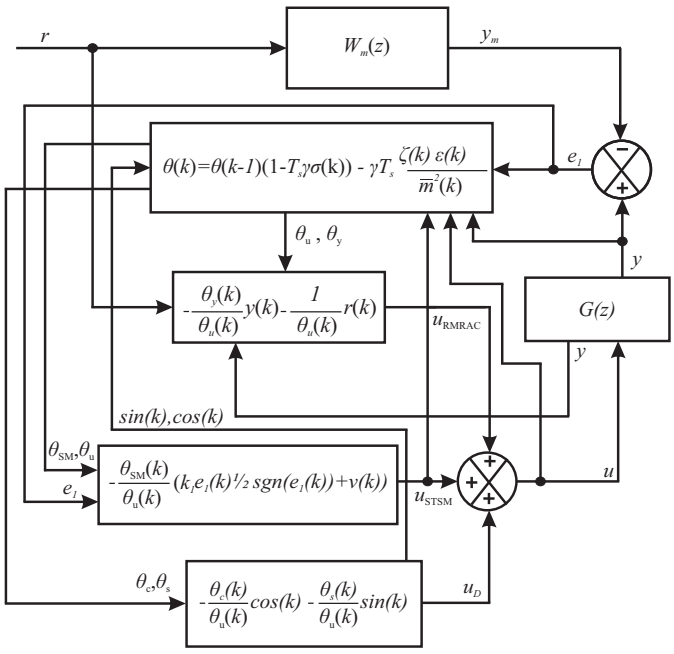

Figure 5. RMRAC-STSM block diagram.

The adaptive control law regarding the periodic disturbance imposed by the electrical grid voltage v_d is

$$u_D(k) = -\frac{\theta_c(k)}{\theta_u(k)}cos(k) - \frac{\theta_s(k)}{\theta_u(k)}sin(k). \tag{14}$$

Then, the complete control law can be rewritten as the sum of three terms: RMRAC (u_{RMRAC}), STSM (u_{STSM}) and periodic disturbance (u_D),

$$u(k) = u_{RMRAC}(k) + u_{STSM}(k) + u_D(k). \tag{15}$$

Figure 5 presents the block diagram from RMRAC-STSM structure considering the electrical grid dynamic modeled as a periodic disturbance.

D. Steps for RMRAC-STSM algorithm implementation

Once the discrete equations of the controller and the reference model used have been defined, a roadmap for implementing the control structure can be made, as follows:

1) Reference update: $r(k)$;
2) Reference model output update: $y_m(k)$;
3) Tracking error update: $e_1(k)$;
4) Control law update: $u(k)$;
5) Aguilar filter update: $\boldsymbol{\zeta}(k)$;
6) Majorant signal update: $m^2(k)$;
7) Augmented error update: $\epsilon(k)$;
8) Adaptive parameter vector update: $\boldsymbol{\theta}(k)$.

IV. Control Application

The proposed RMRAC-STSM control structure was applied to current control of a three-phase grid-tied VSI with LCL filter using a TMS320F28335 DSP and a *Typhoon*© HIL 402. The use of HIL has been shown to be effective to validate control structures, considering that it is possible to

modify plant parameters, controllers and add disturbances to the system in real time [18].

A. Steps of Realized Experiment

The test is started with bus voltage $V_{link} = 500V$ and the AC line voltage is set to $220V$. The sampling and switching frequency is $5040Hz$, while the data storage frequency of the DSP is $333Hz$, that is, during interruptions of the control system the microcontroller saves in memory 1 every 25 samples processed. This strategy was adopted considering hardware limitation in order to obtain sufficient data to adequately assess the parametric convergence of the control system.

In addition, normalized voltages in α and β coordinates are estimated using the *Kalman* filter proposed in [15]. After synchronization with the electrical grid, the signals sampled by the DSP begin to be stored in memory and the instant $t = 0s$ is established, and then there is the following steps:

1) The three-phase injected currents (i_{Lg}) reference were set to $5A_{pk}$ until $t = 0,1002s$;
2) At $t = 0.1002s$ a load step is performed and i_{Lg} reference is updated to $10A_{pk}$;
3) At $t = 0.2004s$, i_{Lg} reference is set to $20A_{pk}$;
4) When $t = 0.4008s$, the grid injected currents reference are updated again to $30A_{pk}$ (full load);
5) At $t = 0.8016s$ a disturbance is inserted in the grid with $L_{g2} = 1mH$ in order to verify the performance of the controller in an environment that simulates a weak grid.
6) When $t = 1.2024s$ the experiment is finished.

B. HIL Results using RMRAC-STSM

The following parameters were used to implement the RMRAC-STSM control structure for VSI three-phase current regulation: $k1 = 1$, $k2 = 1$, $\Gamma = 10000$, $G = 200$ and $\boldsymbol{\theta} = [\ 1\ \ 0.98\ \ 1.6\ \ 0.99\ \ 2.3\ ]^T$. The majorant gain ($G$) and the adaptation gain (γ) were chosen so that the ratio between the majorant and adaptation gain is at least 10 times, ensuring a fast dynamic response for the adaptive system. As for the initial values of the adaptation parameter vector $\boldsymbol{\theta}$, these values were taken from a previous simulation, already close to their convergence. $k1$ and $k2$ were set to 1, since STSM is adaptive.

Figure 6 shows the currents injected into the electrical grid by the VSI converter, in abc coordinates, when it is possible to observe that the RMRAC-STSM structure can regulate the system with low overshoots during load variations ($t = 0.1002s$, $t = 0.2004s$ and $t = 0.4008s$). In addition, when there was added a $L_{g2} = 1mH$ ($t = 0.8016s$), representing a weak grid environment, the currents were disturbed for a short transient, but the control system acted fast to find a new set of parameters in order to keep the system stable.

In addition, Figure 7 presents the tracking error e_1, in $\alpha\beta$ coordinates. It is possible to observe in Figure 7 that e_1 amplitude is disturbed during the imposed variations on plant, but oscillates around zero in steady state. Also, the tracking error presents no high frequency oscillation (chattering).

Figure 8 shows the RMRAC-STSM control laws in $\alpha\beta$ coordinates. Based on Figure 8, it can be noted that u_{RMRAC}

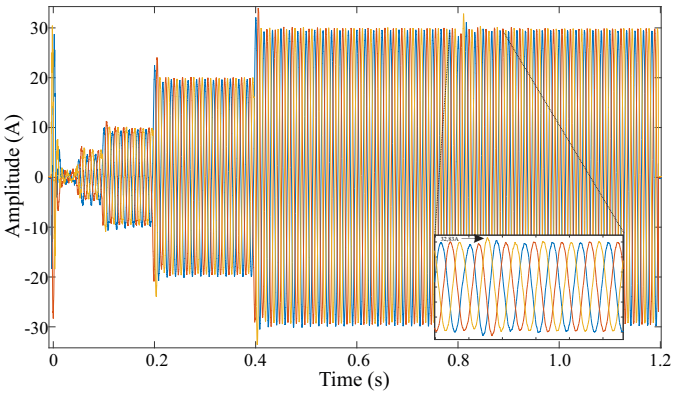

Figure 6. Three-phase electrical grid injected currents in abc coordinates.

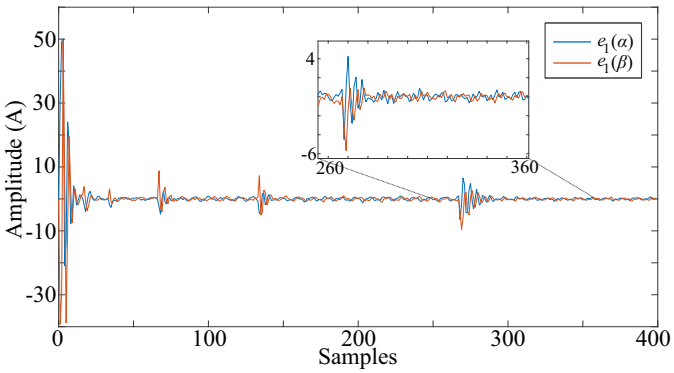

Figure 7. Currents tracking error (e_1) in $\alpha\beta$ coordinates.

and u_{STSM} are significantly disturbed when the system suffered load steps and inductance addition, but u_{RMRAC} rapidly follows the new reference and u_{STSM} acts more intense during transients, tending to zero in steady state, eliminating the chattering presence from SM action. Moreover, it did not saturate in any instant of the test, neither bursting phenomenon occurred. Also, Figure 9 presents the adaptive gains $\boldsymbol{\theta}$ in $\alpha\beta$ coordinates. It can be noted that the adaptive gains were severely disturbed considering the load steps and inductance addition, but all parameters converged in steady state and no parameters drifting occurs.

V. Conclusion

This paper presented the development of a discrete-time RMRAC-STSM controller applied for current control of a three-phase grid-tied VSI converter with LCL filter. The RMRAC-STSM structure was modeled based on a reduced order LCL filter model and were tested under a weak grid condition. It was observed that the RMRAC-STSM structure presented good regulation performance and low tracking error in steady state. Also, there was a considerable effort of control actions considering the disturbances imposed to the plant, where the control action u_{STSM} made a significant contribution during the transitional periods, with its activity tending to zero when the system entered in steady state. Therefore, the RMRAC-STSM controller behaved robustly to imposed disturbances and unmodeled dynamics, where all adaptive parameters converged, keeping the system well

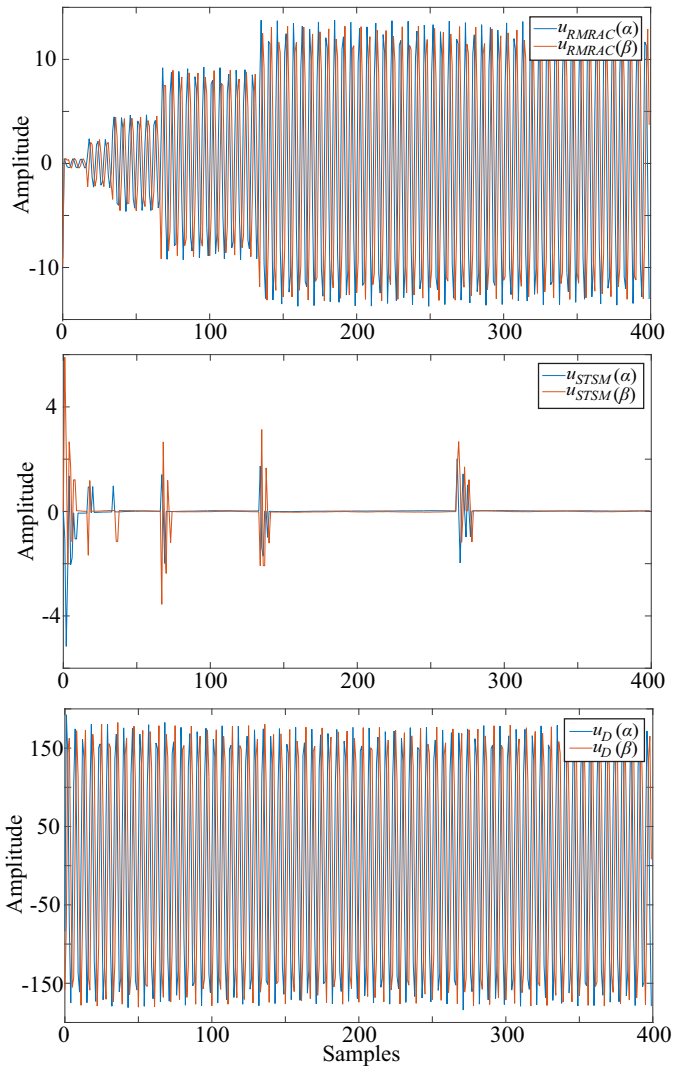

Figure 8. RMRAC-STSM control laws in $\alpha\beta$ coordinates.

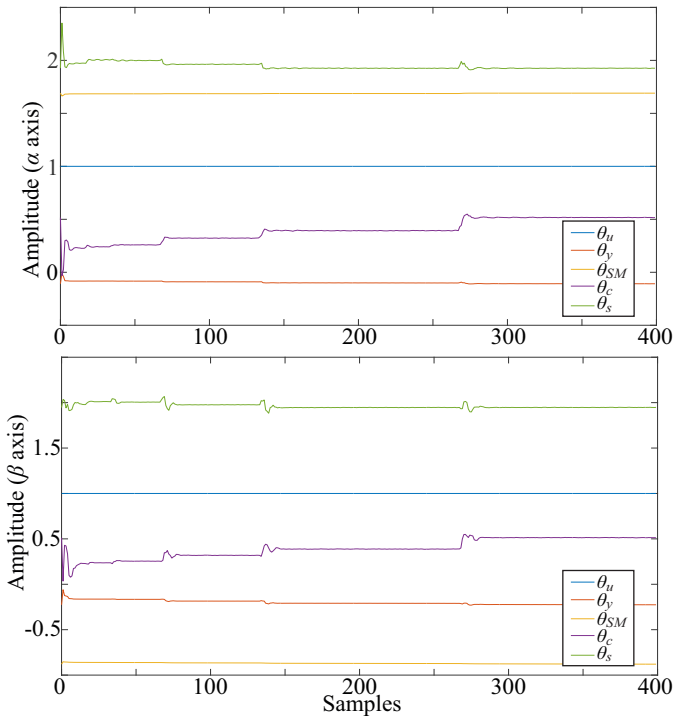

Figure 9. Adaptation gains ($\boldsymbol{\theta}$) in $\alpha\beta$ coordinates.

regulated, presenting itself as a viable alternative for current regulation of three-phase grid-tied converters with LCL filter.

Acknowledgment

This study was financed in part by the Coordenação de Aperfeiçoamento de Pessoal de Nível Superior – Brasil (CAPES/PROEX) – Finance Code 001.

References

[1] Gungor, Vehbi C., et al. "Smart grid technologies:Commu. technologies and standards."IEEE Trans. on Indust. Inform. 7.4 (2011): 529-539.

[2] Liserre, Marco, Frede Blaabjerg, and Steffan Hansen. "Design and control of an LCL-filter-based three-phase active rectifier." IEEE Transactions on industry applications 41.5 (2005): 1281-1291.

[3] M. Lindgren and J. Svensson, 'Control of a voltage-source converter connected to the grid through an LCL-filter-application to active filter', in Proc. of PESC'98, May 1998, vol. I, pg. 229-2315.

[4] Massing, J. R., Stefanello, M., Gründling, H. A., and Pinheiro, H., Adaptive Current Control for Grid-Connected Converters with LCL Filter, IEEE Trans. On Industrial Elect., 2012, 59, (12), pg. 4681-4693.

[5] Alenius, H., Modeling and Electrical Emulation of Grid Impedance for Stability Studies of Grid-Connected Converters, Master Thesis, Tampere University of Technology, 2018.

[6] M. Liserre, et. al., "Stability of Photovoltaic and Wind Turbine Grid-Connected Inverters for a Large Set of Grid Impedance Values", IEEE Trans. on Power Elect., vol. 21, no. 1, pg. 263–272, 2006.

[7] I. J. Gabe, V. F. Montagner, and H. Pinheiro, Design and implementation of a robust current controller for VSI conn. to the grid through an LCL filter, IEEE Trans. On Power Elect., vol.24, no.6, pg.1444–1452, 2009.

[8] Tambara, R. V., Massing, J. R., Pinheiro, H. and Gründling, H. A., A digital RMRAC controller based on a modified RLS algorithm applied to the control of the output currents of an LCL-filter connected to the grid, 15th European Conf. on Power Elect. and Applications (EPE), 2013.

[9] Martins, Leandro Tomé, et al. "Current control of grid-tied LCL-VSI with a sliding mode controller in a multiloop approach." IEEE Transactions on Power Electronics 34.12 (2019): 12356-12367.

[10] Levant, Arie. "Higher-order sliding modes, differentiation and output-feedback control." Intern. journal of Control 76.9-10 (2003): 924-941.

[11] Msaddek, A., Gaalou, A., M'sahli, F., Comparative study of higher order sliding mode controllers, 15th Intern. Conf. on Sciences and Techniques of Automatic Control and Computer Eng. (STA), 2014.

[12] Guo, B., Su, M., Sun, Y., et al., A Robust Second-Order Sliding Mode Control for Single-Phase Photovoltaic Grid-Connected Voltage Source Inverter, in IEEE Acess, vol. 7, pg. 53202 - 53212, 2019.

[13] Bouyahia, Semcheddine, et al. "An adaptive super-twisting sliding mode algorithm for robust control of a biotechnological process." International Journal of Dynamics and Control (2019): 1-11.

[14] Evald, P. J. D. O., Tambara, R. V. and Gründling, H. A., "A Direct Discrete-Time Reduced Order Robust Model Reference Adaptive Control for Grid-Tied Power Converters with LCL filter", Revista Eletrônica de Potência, vol. 25, no 3, pg 1-12, 2020.

[15] Cardoso, Rafael, et al. "Kalman filter based synchronisation methods." IET gen., transm. & distrib. 2.4 (2008): 542-555.

[16] Erickson, Robert W., and Dragan Maksimovic. Fundamentals of power electronics. Springer Science & Business Media, 2007.

[17] Ioannou, P., Tsakalis, K., A robust discrete-time adaptive controller, in 25th IEEE Conference on Decision and Control, 1986.

[18] Bojoi, R., Profumo, F., Griva, G., et al, Advanced research and education in electrical drives by using digital real-time hardware-in-the-loop simulation, Master Thesis, Proc. of Power Electronics and Motion Control Conf. and Exposition (PEMC), Dubrovnik, Croatia, 2002.